Scattered Light in the IUE Spectra of ϵ Aurigae

Bruce Altner
Applied Research Corportation

Robert D. Chapman and Yoji Kondo
Laboratory for Astronomy and Solar Physics
NASA Goddard Space Flight Center

Robert E. Stencel
Astrophysics Division
NASA Headquarters

1. Introduction

Observations of the ϵ Aurigae system early in the International Ultraviolet Explorer (IUE) program revealed an apparent UV excess shortward of 1500Å which was interpreted as the contribution of a hot dwarf companion (Hack and Selvelli 1979). Further observation, both before and during the ensuing eclipse cycle, revealed that the source of the UV excess was highly variable (Boehm, Ferluga and Hack 1984). However, as demonstrated by several researchers (Clarke 1981; Crivellari and Praderie 1982; Basri, Clarke, and Haisch 1985, hereafter BCH) the IUE cross-disperser grating acts to redistribute a measurable percentage of the longer wavelength light into the range of the short wavelength prime (SWP) camera, causing errors in both line and continuum flux levels in the uncorrected spectra.

There have been earlier attempts to correct the ϵ Aurigae IUE spectra for scattered light. Hack and Selvelli (1979) subtracted 500 flux units (FN) from the entire spectrum, treating the scattering as if it were a uniform background contamination, independent of wavelength. Parthasarathay and Lambert (1983) also recognized that scattered light might be important in establishing the properties, and indeed the very existence, of a hot companion. They used the descattering methods suggested by Clarke (1981) and Crivellari et al. (1980) and concluded that the signal shortward of 1250 Å was purely scattered light. They also suggested several alternatives to the hot companion model for the remaining UV excess shortward of 1600 Å (see section 4).

It is clearly of crucial importance to our understanding of the nature of the UV excess that we carefully evaluate the level of scattered light contributing to it. In order to do so we have applied the BCH algorithm to a number of low dispersion IUE spectra of ϵ Aurigae from very early pre-eclipse through the most recent post-eclipse epochs. As noted in BCH, scattered light is most significant when there is a great deal of contrast

between adjacent spectral regions. Indeed, ϵ Aurigae has such a spectrum, being of the same spectral type as Canopus, the star chosen by BCH as the best candidate for their scattered light study.

We have found that the IUE spectra vary on timescales comparable to the optical photometry (Schmidtke 1985) in agreement with Ake (1985) and that they are indeed partially contaminated by scattered light. Even after correction for this instrumental effect, however, a significant, time dependent UV excess is still present.

2. Data Reduction and the Descattering Procedure

The BCH correction for scattered light in IUE spectra goes beyond the earlier work mentioned above in being more general and is therefore of wider applicability. The authors determined a "best fit" empirical scattering profile for the cross-disperser grating by convolving an assumed scattering profile with a "true" Canopus spectrum and comparing the result to various IUE images of this F0 Ib-II star. The "true" Canopus consisted of a Kurucz (1979) model (T_{eff} = 7500 K, log g = 2.0 and log A = 0.0) except in the spectral range $1420 < \lambda < 3440$, where TD-1 and OAO II fluxes were used. The adopted scattering profile was derived from results of tests on a replica of a grating made from the same master as that used to produce the one actually flown aboard IUE (Mount and Fastie 1978). The profile was modified to include scattering from the cores of emission lines and extended by adding exponentially decreasing wings. Four free parameters are needed to describe these modifications to the Mount and Fastie profile. The interested reader is referred to the BCH paper for more details of these parameters and the errors associated with their determination.

Once the best fit profile is determined it can be deconvolved from any IUE spectrum to return a "descattered" spectrum, and this is the approach that we used. The default, normalized scattering profile assumes a level of 4% scattering from a bin at the reference wavelength (arbitrarily selected at the midpoint of the combined short and long wavelength range) as one of the four parameters. That light is then redistributed to all other wavelengths in accordance with the shape of the adopted profile. For other than the reference bin the efficiency scales as $(\lambda_{ref}/\lambda)^2$. Hence, a value of 4% at 2450 implies a 16% scattering efficiency in the region of the Lyman α line.

Because the light scattered into the range of the SWP camera originates from longer wavelengths, we have merged all SWP spectra with LWR or LWP observations taken on the same day. The spectra input into our subsequent procedures are absolutely calibrated fluxes from the SWP camera for $\lambda \lesssim$ 1950 Å and from the LWR or LWP cameras at $\lambda \gtrsim$ 1950 Å, yielding an effective wavelength coverage of $1150 \lesssim \lambda \lesssim 3350$ Å. We have applied the absolute calibration of Bohlin and Holm (1980) to the SWP and LWR spectra and that of Cassatella and Harris (1982) to the LWP images. In addition, we have used the correction suggested by Holm, et al. (1982) for errors due to variations in the camera head amplifier temperature.

The BCH procedure was originally designed to work with input data in 5 Å steps, wider bins being inappropriate for spectral *line* studies. Our primary concern in this work is the short wavelength *continuum*; hence we are not similarly restricted. Moreover, the signal/noise is quite poor in certain spectral intervals of key importance, i.e., $1150 \lesssim \lambda \lesssim 1550$ Å (the region which purportedly shows a UV excess but which has the smallest intrinsic SWP flux) and $2000 \lesssim \lambda \lesssim 2400$ (the "nearest" region of the long wavelength spectrum and hence the most sensitive to the actual shape of the redistribution function for scattering into the short wavelength region). Therefore, we averaged the data in 50 Å wide bins, appropriately weighted to eliminate reseaux and other flagged points of questionable quality, and modified the original BCH code so as to allow input data of any reasonable bin size.

These merged, absolutely calibrated, binned spectra were then passed to the descattering algorithm. In all cases we have used the "best fit" parameters determined by BCH for the scattering profile, motivated in part by the similarity in spectral type of Canopus and ϵ Aurigae. We have investigated the effect of a twofold reduction in the assumed scattering efficiency, however, in light of some evidence that the 4% value might be too large (c.f., see discussion below).

3. Results and Discussion

Figure 1 depicts the wavelength and time dependence of the scattered light found by the BCH procedure for spectra obtained throughout the eclipse. The quantity plotted is the scattered light fraction, defined as

$$R(\lambda,\Phi) = 100 \times (F^{O}(\lambda,\Phi) - F^{C}(\lambda,\Phi))/F^{O}(\lambda,\Phi)$$

where $F^{O}(\lambda,\Phi)$ = the flux at wavelength λ and eclipse phase Φ, for the uncorrected (input) spectrum, and

$F^{C}(\lambda,\Phi)$ = the flux at wavelength λ and eclipse phase Φ, for the corrected (output) spectrum.

A quadratic interpolation was applied to the data along the phase axis in order to display non-uniformly spaced points on a uniform scale. In most cases the scattered light fraction among the longer wavelength bins is insignificant, whereas for $\lambda \lesssim 1550$ Å $R(\lambda,\Phi)$ increases rapidly. One exception is the region λλ 2000-2400 which, as mentioned above, is the least sensitive portion of the long wavelength cameras.

Without even considering the vertical axis of Figure 1 we can easily detect an interesting facet of the phase dependence of $R(\lambda,\Phi)$ in the short wavelength bins. Not surprisingly, the figure implies that the amount of scattered light is greatest when the star is brightest, i.e., before first contact, after fourth contact and during the mid-totality brightness enhancement. Since we would not expect an uneclipsed hot secondary to show the same time dependence as the eclipsed primary we interpret this result as an independent verification that we are indeed dealing with

scattered light. *Now* if we consider the values along the vertical axis we see that up to 20% of the flux at the short wavelengths is scattered light. Two important questions then arise: 1) how reliable are the assumptions that set the scale of the vertical axis? and 2) what about the flux that *is not* scattered light? We shall consider each question in turn.

In his application of the BCH algorithm to the spectra of comets Feldman (private communication) derived a scattering profile from the shape of an overexposed Lyman α emisssion line. He found an efficiency of scattering from line center of about 2%, compared to the 4% found by BCH. This was partially compensated by a larger fractional scattering into the near wings, important for emission line studies but not for the continuum case under study here. In Figure 2 we show the results of a test comparison of the two cases, 4% and 2% scattering efficiency, for our most recent post-eclipse observation. Although the fractional scattered light is also reduced by the expected factor of two, we note that there is still agreement in the regions of overlapping uncertainty (± 1 σ). Hence, it seems reasonable to consider the 2% case as a *lower limit* to the actual values of $R(\lambda,\Phi)$, for this and all other epochs.

A rough method for estimating the amount of scattered light in an IUE spectrum has recently been suggested by Imhoff (1985). Her empirically derived procedure determines the number of DN per second scattered into the SWP camera range from the long wavelength spectrum at 2400 Å. Since the BCH procedure sums the contribution from the entire long wavelength spectrum it might be expected that the values of $R(\lambda,\Phi)$ derived from it would be larger than those determined from Imhoff's "rule of thumb". However, it is evident from Figure 2 that this is not the case. Even with the rather large uncertainties Imhoff's approximation predicts a larger fractional scattered light than that found using the BCH algorithm. This suggests either that the "rule of thumb" procedure overestimates the scattered light or that the profile adopted by BCH leads to a considerable underestimate. The latter seems unlikely, since the profile was determined from a best fit to a star of the same spectral type as ϵ Aurigae. Lacking further information as to the validity of the assumptions that were made in constructing the BCH profile (i.e., do the far wings really fall off exponentially?) we shall henceforth interpret the larger values derived from the Imhoff procedure as convenient *upper* limits to the full BCH treatment. We shall use the upper limit results in the later figures, in lieu of error bars, to represent the maximum correction for scattered light.

Let us return to the second question posed in the discussion of Figure 1. Having subtracted away the scattered light contribution in each wavelength bin for each of the spectra, we are now in a position to examine the intrinsic UV flux, and note how it behaves as a function of "eclipse phase". Units of eclipse phase are defined such that first contact occurs at $\Phi = 0.00$ and last contact at 1.00, based on dates predicted by Gyldenkerne (1970) for the eclipse in *optical wavelengths*. In these units second contact occurs at $\Phi = 0.200$ and third contact at 0.790.

In Figure 3 we present eclipse light curves, both before and after the scattered light correction, for three representative wavelength bins, 1350,

1450, and 1600 Å. In all cases we plot magnitude versus Φ, defined as

$$m_\lambda(\Phi) = -2.5 \log F_\lambda(\Phi) - 21.1$$

where the constant 21.1 refers to the absolute energy calibration of Vega derived by Hayes and Latham (1975). One can easily show that the difference between the light curve corrected for scattered light and the uncorrected curve is related to the R values discussed above by

$$\delta m_\lambda(\Phi) = m_\lambda^c(\Phi) - m_\lambda^o(\Phi) = -2.5 \log (1 - R(\lambda,\Phi))$$

where R is used here as a fraction, rather than a percentage.

Inspection of Figure 3 demonstrates a number of interesting results. First, it can be easily seen that, with increasing wavelength, the corrected light curves fall closer and closer to the uncorrected curves. For $\lambda > 1700$Å the curves are virtually indistinguishable. This trend is entirely consistent with the result, noted in Figure 1, that the percent scattered light is greatest for the short wavelengths in the SWP camera and approaches zero at the longer wavelengths. Second, we note that the corrected and uncorrected light curves differ most at the "brightest" phases, i.e., before and after the eclipse itself and during those phases associated with the central brightening feature (for those wavelengths where there is still a difference), again in accord with the results of Figure 1. We see that the effect of scattered light is to "fill in" the curve, making it shallower than it should be at the shortest wavelengths. Most notably, it is quite disputable whether or not the curve at 1350 Å is an eclipse curve, especially considering the large uncertainties concomitant with the low intrinsic flux levels.

To address directly the question of the reality of a UV excess in the ϵ Aurigae system we examine the spectra after we have removed the scattered light component. Does evidence for an apparent hot component remain? The answer seems to be "yes". For several of our observations a modest percentage of the UV excess is accounted for once we subtract away the scattered light. In others, almost none of the excess is removed. Figure 4 shows a typical example of the former case, in which subtracting even the upper limit of scattered light does not significantly reduce the UV excess at wavelengths below 1550 Å. The format of Figure 4 is deliberately similar to that used by Hack and Selvelli (1979), the first report of an excess in IUE spectra of ϵ Aurigae to appear in the literature.

When spectra (corrected for scattered light) from several different dates throughout the eclipse are plotted in a manner similar to that used in Figure 4, large variations are seen in slope of the continuum shortward of 1600 Å. Figure 5 is a schematic illustration of the short wavelength variations observed. The fluxes in Figure 5 have all been arbitrarily adjusted to yield the same value at 3300 Å as the model atmosphere of Kurucz (1979) used in Figure 4, a procedure which presumably removes the eclipse time dependence from the data. The time variations that remain are associated either with the eclipse-independent fluctuations of the hot component itself, with gaps or tunnels in the occulting secondary (Wilson

1971; Altner et al. 1984), or with the cepheid-like pulsations of the primary, which can be quite large at short wavelengths (Ake and Simon 1984). Figure 6 shows the data at 1300, 1400 and 1500 Å, adjusted in the same manner, plotted versus time. There is some suggestion of cyclic behavior in the curves, and a detailed study of this time dependence is presently underway.

In early February of 1984 the ultraviolet spectrometer (UVS) aboard the Voyager 1 spacecraft observed ϵ Aurigae (R. Polidan, private communication). The spectrum obtained is consistent with a star of spectral type B5; however, since a known B5 star is close enough to ϵ Aurigae to have been included in the 0.1 degree by 0.9 degree aperture, the identification is suspect. An additional UVS observation is planned, from which it is hoped that the uncertainty in the identification of the UV source will be resolved. Ake and Simon (1984) noted that the *line* spectrum of ϵ Aurigae shortward of 1400 Å does not match that of a B5 star. They concluded from this that whatever the hot component is, it is *not* a hot star, which suggests that the flux observed by the UVS instrument was due to the known B5 star. Nevertheless, the UVS data seems not to be inconsistent with the fluxes in the short wavelength IUE spectrum obtained in mid-February of 1984. We will follow with great interest future UVS observations of ϵ Aurigae, with the intent being to compare the results with future IUE data and U, B, and V photometry.

4. Summary

As a result of this work we have found that light scattered from the longer wavelengths constitutes a small but non-negligible, wavelength and time dependent fraction of the measured flux in the far UV. We have not been able to unambiguously rule out the reality of the UV excess. However, we note that there are still uncertainties in the assumed scattering profile. New measurements of the scattering properties of the cross-disperser grating are planned in order to verify the results of Mount and Fastie (1978) and extend the wavelength coverage into the far wings of the profile (B. Woodgate, private communication). The results of these measurements will no doubt reduce some of these uncertainties. For the present, we feel that the BCH approach is a significant improvement over the methods heretofore available for the treatment of scattered light in IUE spectra.

IUE imposed constraints on the particle size and temperature of the disk surrounding the secondary were first discussed by Castelli et al. (1982) and Chapman et al. (1983). Later infrared results confirmed the prediction that the disk temperature had to be significantly lower than that of the supergiant (Backman et al. 1984). The apparent contradiction inherent in the coexistence of an ultraviolet excess and an infrared temperature around 500 K was one of the primary motivations for undertaking this study. Future observations, such as those possible with the Voyager UVS and other instruments, will undoubtedly gain us new insight into the problem. Of particular interest, in the long term, is observation of the ϵ Aurigae secondary at quadrature and, later still, in eclipse.

Meanwhile, we look to theoretical models which allow both a UV excess and a cold disk, such as star spots on the surface of the primary (Parthasarathy and Lambert 1983), or polar flows associated with a double star embedded in the disk (Lissauer and Backman 1985).

We acknowledge the assistance of the IUE staff in acquiring the spectra of ϵ Aurigae throughout the many months of the eclipse cycle, and of the staff of the Regional Data Analysis Facility at Goddard Space Flight Center, whose helpful advice in reducing the data was an invaluable resource. We are grateful to Dr. G. Basri for providing the FORTRAN code of the BCH procedure and for taking the time to clarify some of the finer points involved in its application.

References

Ake, T.B., and Simon, T. 1984, *Future of Ultraviolet Astronomy Based on Six Years of IUE Research*, Mead, J.M., et al., eds., 361.
Ake, T.B. 1985, in *Workshop on the Recent Eclipse of Epsilon Aurigae*, R.E. Stencel, ed., this volume.
Altner, B., Chapman, R.D., Kondo, Y., and Stencel, R.E. 1984, *Future of Ultraviolet Astronomy Based on Six Years of IUE Research*, Mead, J.M., et al., eds., 365.
Backman, D.E., Becklin, E.E., Cruikshank, D.P., Joyce, R.R, Simon, T., and Tokunga, A. 1984, *Ap. J.*, **284**, 700.
Basri, G., Clarke, J.T., and Haisch, B.M. 1985, *Astr. Ap.*, **144**, 161.
Boehm, C., Ferluga, S., and Hack, M. 1984, *Astr. Ap.*, **130**, 419.
Bohlin, R.C., and Holm, A. 1980, *NASA IUE Newsletter No.* **10**, 37.
Cassatella, A., and Harris, A.W. 1982, *IUE ESA Newsletter*, **17**, 12.
Castelli, F., Hoekstra, R., and Kondo, Y. 1982, *Astr. Ap. Suppl.*, **50**, 233.
Chapman, R.D., Kondo, Y., and Stencel, R.E. 1983, *Ap. J. (Letters)*, **269**, L17.
Clarke, J.T. 1981, *NASA IUE Newsletter No.* **14**, 143.
Crivellari, L., Morossi, C., and Ramella, M. 1980, in *IUE Data Reduction*, W.W. Weiss et al., eds., 185.
Crivellari, L., and Praderie, F. 1982, *Astr. Ap.*, **107**, 75.
Gyldenkerne, K. 1970, *Vistas in Astr.*, **12**, 199.
Hack, M., and Selvelli, P.L. 1979, *Astr. Ap.*, **75**, 316.
Hayes, D., and Latham, D. 1975, *Ap. J.*, **197**, 593.
Holm, A., and Rice, 1981, *NASA IUE Newsletter No.* **15**, 74.
Holm, A., Bohlin, R.C., Cassatella, A., Ponz, D., and Schiffer, F.H. 1982, *Astr. Ap.*, **112**, 341.
Imhoff, C.L. 1985, *NASA IUE Newsletter No.* **26**, 5.
Kurucz, R.L. 1979, *Ap. J. Suppl.*, **32**, 7.
Lissauer, J.J., and Backman, D.E. 1985, *Ap. J.*, in press.
Mount, G.H., and Fastie, W.G. 1978, *Applied Optics*, **17**, 3108.
Parthasarathy, M., and Lambert, D.L. 1983, *Publ. Astr. Soc. Pacific*, **95**, 1012.
Schmidtke, P.C. 1985, in *Workshop on the Recent Eclipse of Epsilon Aurigae*, R.E. Stencel, ed., this volume.
Wilson, R.E. 1971, *Ap. J.*, **170**, 529.

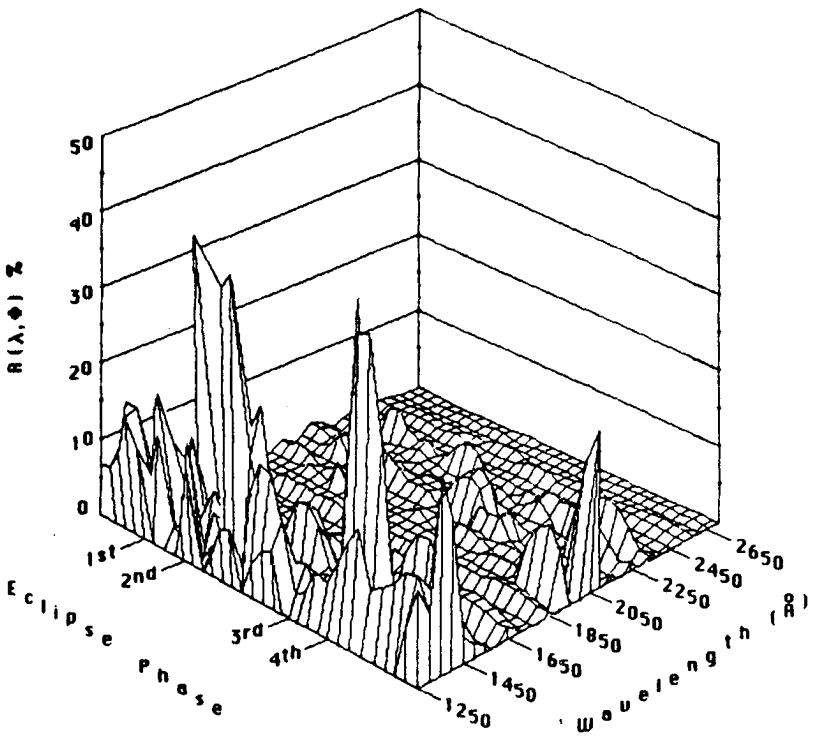

Figure 1

The relative percentage of scattered light in each wavelength bin for each observation (data is interpolated to give uniform spacing in the time coordinate). The tic marks along the phase axis refer to the contact points of the eclipse. An apparent trend toward larger amounts of scattered light during the uneclipsed (i.e., brighter) phases can be seen, as well as during the mid-eclipse brightness enhancement apparent in the light curves. This behavior at the shortest wavelengths is expected if the signal is scattered light.

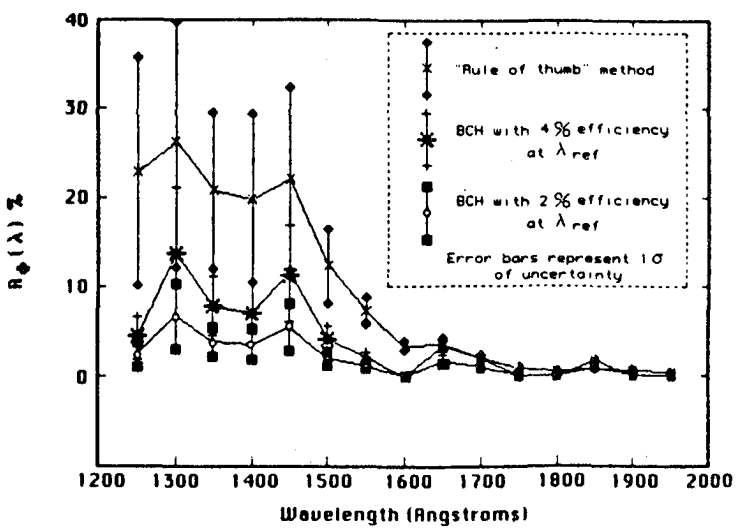

Figure 2

Relative percent scattered light as a function of wavelength for a typical IUE observation of Epsilon Aurigae (Φ_e = 1.434). The effect of varying the scattering efficiency parameter is shown. Although the two cases give percentages which differ by a factor of two, the overlapping uncertainties show that this parameter is not critical, at least for the case of continuum scattering. At its upper limit the 4% case approaches the rough estimate derived using Imhoff's (1985) "rule of thumb".

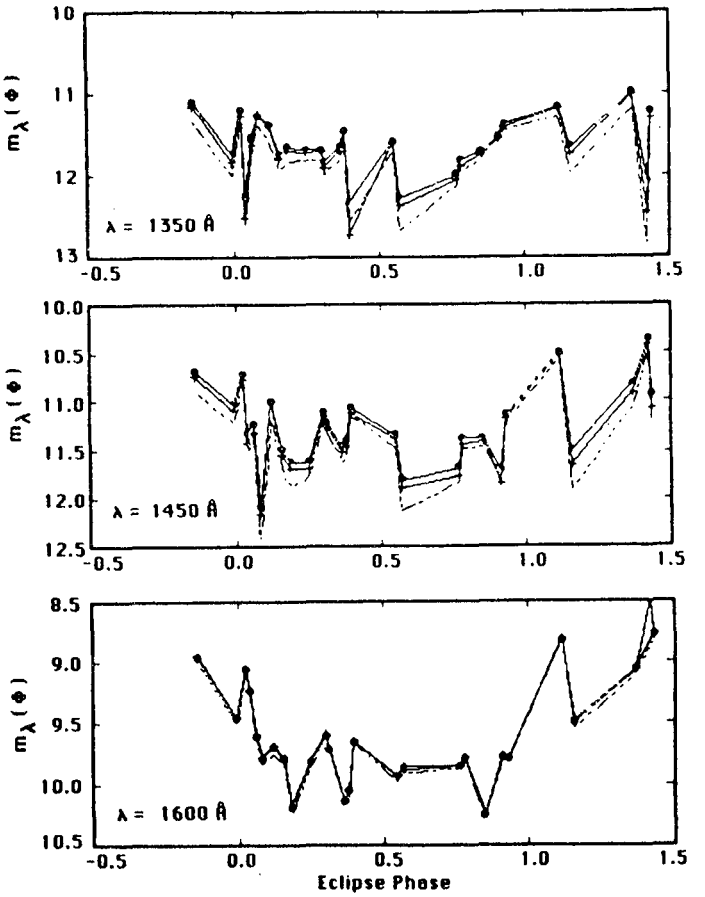

Figure 3

Eclipse light curves for three different wavelength bins. In each case the filled dots represent the uncorrected data while the plus signs are the same data corrected for scattered light using the BCH program with the default parameters, and the dashed line is the curve corrected using the "rule of thumb" method. At wavelengths longward of 1700 Å the three curves are virtually indistinguishable.

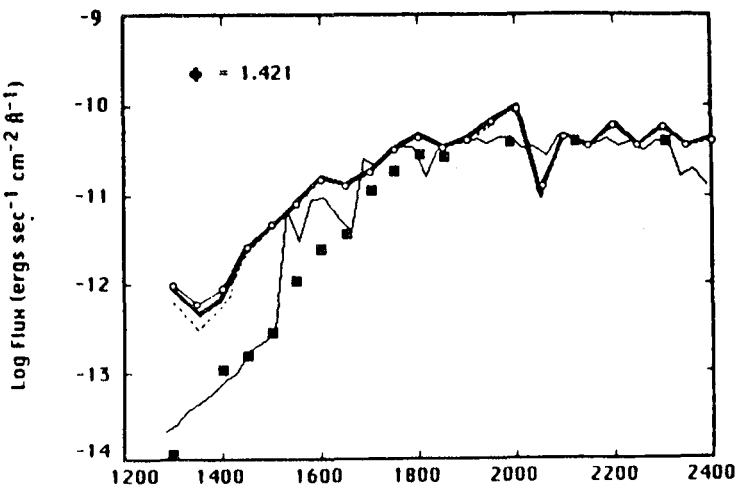

Figure 4

A typical example of the partial reduction in the apparent UV excess after subtracting the scattered light component. The thin line is a Kurucz (1979) model stellar atmosphere with T_{eff} = 7500 K, log g = 1.0, and log A = 0.0, adjusted to the distance and angular diameter of Canopus. The filled squares are the TD-1 and OAO-2 data for Canopus, scaled as in Hack & Selvelli (1979). The spectrum of Epsilon Aurigae well outside of eclipse is shown by the remaining curves. Open circles: no correction for scattered light. heavy line: correction using the BCH code with default paramters, dotted line: correction using Imhoff's "rule of thumb" estimate.

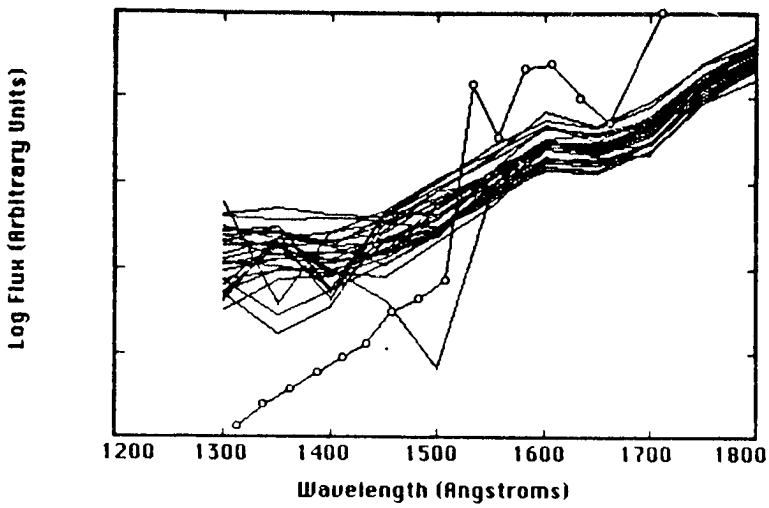

Figure 5

A demonstration of the time variation of the short wavelength spectra with variations due to the eclipse "filtered out" by adjusting all the continua to the value of the Kurucz (1979) model (open circles; same model as used in the previous figure) at 3300 Å. At the extreme short wavelength end, the variations range over almost 2 magnitudes.

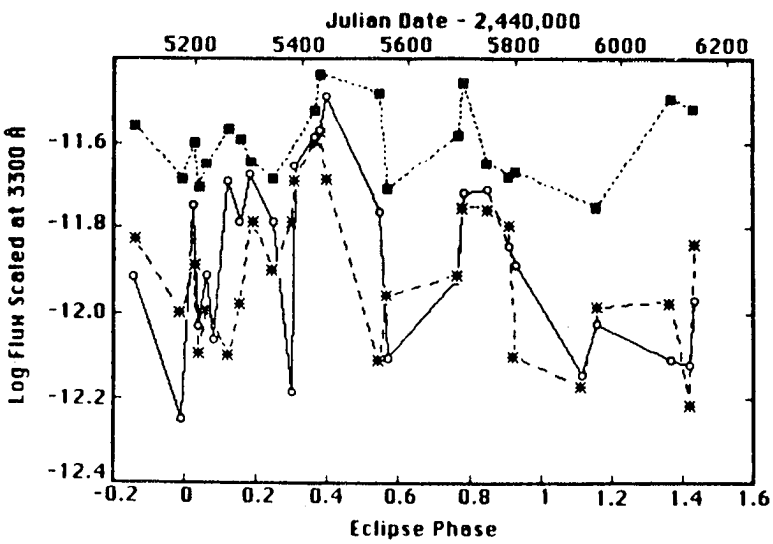

Figure 6

Logarithm of the Epsilon Aurigae fluxes, corrected for scattered light and adjusted to the same value at 3300 Å, as a function of time. By scaling the fluxes in the near UV the time variation due to the eclipse is suppressed, leaving evidence of another time dependence, associated either with the UV excess itself or with the cepheid-like pulsations of the primary. Open circles 1300 Å, asterisks 1400 Å, filled squares 1500 Å.